Robust stabilization of a fully actuated 3D bipedal locomotion via nonlinear H ∞ -control under unilateral constraints

Oscar Eduardo Montaño Godinez, Yuri Orlov, Yannick Aoustin, Christine Chevallereau

Robust stabilization of a fully actuated 3D bipedal locomotion via nonlinear $\mathcal{H}_\infty$-control under unilateral constraints

Oscar Montano, Yury Orlov, Yannick Aoustin, Christine Chevallereau

***Abstract*— The applicability of the $\mathcal{H}_\infty$ control technique to a fully actuated 3D biped robot is addressed. In contrast to previous studies, this investigation contributes to the study of robustness of bipedal locomotion while assuming an imperfect knowledge of the restitution rule at the collision time instants in addition to external disturbance forces applied during the single support phases. Performance issues are illustrated on a numerical study performed on the 32-DOF biped robot ROMEO, of Aldebaran Robotics.**

I. Introduction

The study of mechanical legged locomotion has been motivated by its potential use as means of locomotion in rough terrains, but in particular, the interest arises from diverse sociological and commercial interests, ranging from the desire to replace humans in hazardous occupations (demining, nuclear power plant inspection, military interventions, etc.), to the restoration of motion in the disabled [1].

For practical implementation, a good mechanical design and a good modeling, play a very important role in achieving good performance. However, in real world applications, bipedal robots are subject to many sources of uncertainty during walking; these could include a push from a human, an unexpected gust of wind, geometric perturbations of the terrain heights, or parametric uncertainties of non-modeled friction forces [2]. For these reasons, the design of feedback control systems, capable of attenuating the effect of these uncertainties is critical to achieve the desired walking gait.

The complete model of the biped robot considered in this work is simplified as a hybrid system consisting of free-motion phases separated by impacts. The study of hybrid dynamical systems has recently attracted a significant research interest, basically, due to the wide variety of applications and the complexity that arises from the analysis of this type of systems (see, e.g. [3], [4], and references quoted therein). Particularly, the disturbance attenuation problem for hybrid dynamical systems has been addressed by [5], [6], where impulsive control inputs were admitted to counteract/compensate disturbances/uncertainties at time instants of instantaneous changes of the underlying state. It should be noted, however, that in addition to the complexity of finding a solution that the equations that allow the synthesis of the control law, the physical implementation of impulsive control inputs is impossible in many practical situations, e.g., while controlling walking biped robots.

Other robust control techniques, such as sliding modes control, have been designed for this kind of systems (see *e.g.*, the works by [7], [8], [9], [10]. While providing both finite-time convergence to a desired reference trajectory and disturbance rejection, these approaches also entail the well-known problem of chattering in the actuators. This further motivates the study of robust control techniques such as the one presented in this work, which attenuate the effect of disturbances while avoiding undesirable and harmful effects on both the actuators, and the joints.

Hence, the present investigation studies the applicability of the $\mathcal{H}_\infty$ control technique, recently extended in [11] towards mechanical systems operating under unilateral constraints, to the 32 degrees-of-freedom biped robot ROMEO, of Aldebaran Robotics [12]. In contrast to previous studies, this investigation contributes to the study of robustness of bipedal locomotion while assuming an imperfect knowledge of the restitution rule at the collision time instants in addition to external disturbance forces applied during the single support phases.

The paper is outlined as follows. Section 2 presents background materials on $\mathcal{H}_\infty$-control under unilateral constraints. Capabilities of the presented state feedback synthesis are illustrated in Sect. 3 in a numerical study of the robust trajectory tracking of a 3D biped robot with feet required to track a walking gait composed of single support phases separated by impacts. Finally, conclusions of this work are presented in Sect. 4.

II. Background materials

In this section, the $\mathcal{H}_\infty$ control problem under unilateral constraints is stated, and sufficient conditions for the existence of a solution are presented. Later on, the applicability of these results on the biped robot of interest will be studied.

A. Problem Statement

Given a scalar unilateral constraint $\mathbf{F}(\mathbf{x_1}, t) \geq 0$, consider a nonlinear system, evolving within the above constraint, which is governed by continuous dynamics of the form

$$\begin{aligned} \dot{\mathbf{x}}_1 &= \mathbf{x}_2 \\ \dot{\mathbf{x}}_2 &= \mathbf{\Phi}(\mathbf{x}_1, \mathbf{x}_2, t) + \mathbf{\Psi}_1(\mathbf{x}_1, \mathbf{x}_2, t)\mathbf{w} + \mathbf{\Psi}_2(\mathbf{x}_1, \mathbf{x}_2, t)\mathbf{u} \end{aligned} \tag{1}$$

$$\mathbf{z} = \mathbf{h_1}(\mathbf{x}_1, \mathbf{x}_2, t) + \mathbf{k_{12}}(\mathbf{x}_1, \mathbf{x}_2, t)\mathbf{u} \tag{2}$$

beyond the surface $\mathbf{F}(\mathbf{x_1}, t) = 0$ when the constraint is inactive, and by the algebraic relations

$$\begin{aligned} \mathbf{x}_1(t_i^+) &= \mathbf{x}_1(t_i^-) \\ \mathbf{x}_2(t_i^+) &= \mu_0(\mathbf{x}_1(t_i), \mathbf{x}_2(t_i^-), t_i) + \omega(\mathbf{x}_1(t_i), \mathbf{x}_2(t_i^-), t_i)\mathbf{w_d^i} \end{aligned} \tag{3}$$

$$\mathbf{z_i^d} = \mathbf{x}_2(t_i^+) \tag{4}$$

at *a priori* unknown collision time instants $t = t_i,\ i = 1, 2, \ldots,$ when the system trajectory hits the surface $\mathbf{F}(\mathbf{x_1}, t) = 0$. In the above relations, $\mathbf{x}^\top = [\mathbf{x}_1^\top, \mathbf{x}_2^\top] \in \mathbb{R}^{2n}$ represents the state vector with components $\mathbf{x}_1 \in \mathbb{R}^n$ and $\mathbf{x}_2 \in \mathbb{R}^n$; $\mathbf{u} \in \mathbb{R}^n$ is the control input of dimension n; $\mathbf{w} \in \mathbb{R}^l$ and $\mathbf{w_d^i} \in \mathbb{R}^q$ collect exogenous signals affecting the motion of the system (external forces, including impulsive ones, as well as model imperfections). The variable $\mathbf{z} \in \mathbb{R}^s$ represents a continuous time component of the system output to be controlled whereas the post-impact value of the only state component $\mathbf{x}_2(t)$ subjected to the instantaneous change is pre-specified as a discrete component $\mathbf{z_i^d}$ of the to-be-controlled output. The overall system in the closed-loop should be dissipative with respect to the output thus specified. Throughout, the functions $\mathbf{\Phi}$, $\mathbf{\Psi_1}$, $\mathbf{\Psi}_2$, $\mathbf{h_1}$, $\mathbf{k_{12}}$, $\mathbf{F}$, μ_0, and ω are of appropriate dimensions, which are continuously differentiable in their arguments and uniformly bounded in t. The origin is assumed to be an equilibrium of the unforced system (1)-(4), which is located beyond the unilateral constraint, i.e., $F(0,t) \neq 0$, $\mathbf{\Phi}(0,0,t) = 0$, $\mathbf{h_1}(0,0,t) = 0$, for all t and $\mu_0(0,0,0) = 0$.

Admitting the above time-varying representation is particularly invoked to deal with tracking problems where the plant description is given in terms of the state deviation from the reference trajectory to track [13]. Therefore, if interpreted in terms of mechanical systems, equation (1) describes the continuous dynamics before the underlying system hits the reset surface $\mathbf{F}(\mathbf{x}_1, t) = 0$, depending on the position error $\mathbf{x_1}$ only, whilst the restitution law, given by equation (3), is a physical law for the instantaneous change of the velocity error when the resetting surface is hit.

Consider a causal feedback controller

$$\mathbf{u} = \kappa(\mathbf{x}, t) \tag{5}$$

with the function $\kappa(\mathbf{x}, t)$ of class C^1 such that $\kappa(0,t) = 0$. Such a controller is said to be a locally (globally) *admissible controller* iff the undisturbed ($\mathbf{w}, \mathbf{w_d^i} = \mathbf{0}$) closed-loop system (1)–(4) is uniformly (globally) asymptotically stable.

The $\mathcal{H}_\infty$-control problem of interest consists in finding an admissible global controller (if any) such that the $\mathcal{L}_2$-gain of the disturbed system (1)–(4) is less than a certain attenuation level $\gamma > 0$, that is the inequality

$$\int_{t_0}^{T} \|\mathbf{z}\|^2 \mathrm{d}t + \sum_{i=1}^{N_T} \|\mathbf{z_i^d}\|^2 \leq \gamma^2 \left[\int_{t_0}^{T} \|\mathbf{w}\|^2 \mathrm{d}t + \sum_{i=1}^{N_T} \|\mathbf{w_d^i}\|^2 \right] + \sum_{j=0}^{N} \beta_j(\mathbf{x}(t_j^-), t_j) \tag{6}$$

locally holds for some positive definite functions $\beta_j(\mathbf{x}, t)$, $j = 0, \ldots, N_T$, for all segments $[t_0, T]$ and a natural N_T such that $t_{N_T} \leq T < t_{N_T+1}$, and for all piecewise continuous disturbances $\mathbf{w}(t)$ and discrete ones $\mathbf{w_d^i},\ i = 1, 2, \ldots$. In turn, a locally admissible controller (5) is said to be a local solution of the $\mathcal{H}_\infty$-control problem if there exists a neighborhood $\mathcal{U} \in \mathbb{R}^{2n}$ of the origin, validating inequality (6) for some positive definite functions $\beta_j(\mathbf{x}, t), j = 0, \ldots, N_T$, for all segments $[t_0, T]$ and a natural N_T such that $t_{N_T} \leq T < t_{N_T+1}$, for all piecewise continuous disturbances $\mathbf{w}(t)$ and discrete ones $\mathbf{w_d^i},\ i = 1, 2, \ldots$, for which the state trajectory of the closed-loop system starting from an initial point $(\mathbf{x}(t_0) = \mathbf{x_0}) \in \mathcal{U}$ remains in $\mathcal{U}$ for all $t \in [t_0, T]$.

In mechanical terms, for the disturbed case, even if the output $\mathbf{z}$ is not driven to zero, the $\mathcal{L}_2$-gain of the system is still locally less than the specified value γ, so the output will be bounded around zero and in consequence the state trajectories of the plant will evolve around the trajectory to track.

B. Background on Nonlinear $\mathcal{H}_\infty$-Control Synthesis under Unilateral Constraints

For later use, the continuous dynamics (1) are rewritten in the form

$$\dot{\mathbf{x}} = \mathbf{f}(\mathbf{x}, t) + \mathbf{g_1}(\mathbf{x}, t)\mathbf{w} + \mathbf{g_2}(\mathbf{x}, t)\mathbf{u} \tag{7}$$

whereas the restitution rule is represented as follows

$$\mathbf{x}(t_i^+) = \mu(\mathbf{x}(t_i^-), t_i) + \Omega(\mathbf{x}(t_i^-), t_i)\mathbf{w_d^i},\ i = 1, 2, \ldots \tag{8}$$

with $\mathbf{x}^\top = [\mathbf{x}_1^\top, \mathbf{x}_2^\top]$, $\mathbf{f}^\top(\mathbf{x}, t) = [\mathbf{x}_2^\top, \mathbf{\Phi}^\top(\mathbf{x}, t)]$, $\mathbf{g_1}^\top(\mathbf{x}, t) = [\mathbf{0}, \mathbf{\Psi}_1^\top(\mathbf{x}, t)]$, $\mathbf{g}_2^\top(\mathbf{x}, t) = [\mathbf{0}, \mathbf{\Psi}_2^\top(\mathbf{x}, t)]$, $\mu^\top(\mathbf{x}, t) = [\mathbf{x}_1^\top, \mu_0^\top(\mathbf{x}, t)]$, and $\Omega^\top(\mathbf{x}, t) = [\mathbf{0}, \omega(\mathbf{x}, \mathbf{t})]$. In order to simplify the synthesis to be developed and to provide reasonable expressions for the controller design, the following assumptions

$$\mathbf{h_1}^\top \mathbf{k_{12}} = \mathbf{0},\ \mathbf{k_{12}}^\top \mathbf{k_{12}} = \mathbf{I} \tag{9}$$

which are standard in the literature (see, e.g., [14]) are made. Relaxing these assumptions is indeed possible, but it would substantially complicate the formulas to be worked out.

C. Local state-space solution

To present a local solution to the problem in question the underlying system is linearized to

$$\dot{\mathbf{x}} = \mathbf{A}(t)\mathbf{x} + \mathbf{B_1}(t)\mathbf{w} + \mathbf{B_2}(t)\mathbf{u}, \tag{10}$$

$$\mathbf{z} = \mathbf{C_1}(t)\mathbf{x} + \mathbf{D_{12}}(t)\mathbf{u}, \tag{11}$$

within impact-free time intervals (t_{i-1}, t_i) where t_0 is the initial time instant and $t_i,\ i = 1, 2, \ldots$ are the collision time instants, whereas $\mathbf{A}(t) = \left.\dfrac{\partial \mathbf{f}}{\partial \mathbf{x}}\right|_{\mathbf{x}=\mathbf{0}}$, $\mathbf{B_1}(t) = \mathbf{g_1}(0,t)$, $\mathbf{B_2}(t) = \mathbf{g_2}(0,t)$, $\mathbf{C}(t) = \left.\dfrac{\partial \mathbf{h}}{\partial \mathbf{x}}\right|_{\mathbf{x}=\mathbf{0}}$, $\mathbf{D_{12}}(t) = \mathbf{k_{12}}(0,t)$.

By the time-varying strict bounded real lemma [15, p.46], the following condition is necessary and sufficient for the linear $\mathcal{H}_\infty$ control problem (10)-(11) to possess a solution: given $\gamma > 0$,

C1) there exists a positive constant ε_0 such that the differential Riccati equation

$$-\dot{\mathbf{P}}_\varepsilon(t) = \mathbf{P}_\varepsilon(t)\mathbf{A}(t) + \mathbf{A}^\top(t)\mathbf{P}_\varepsilon(t) + \mathbf{C_1}^\top(t)\mathbf{C_1}(t) + \mathbf{P}_\varepsilon(t)[\frac{1}{\gamma^2}\mathbf{B_1}\mathbf{B_1}^\top - \mathbf{B_2}\mathbf{B_2}^\top](t)\mathbf{P}_\varepsilon(t) + \varepsilon\mathbf{I} \tag{12}$$

has a uniformly bounded symmetric positive definite solution $\mathbf{P}_\varepsilon(t)$ for each $\varepsilon \in (0, \varepsilon_0)$;

In order to insure dissipation at the impact times, the following conditions are also considered:

C2) the norm of the matrix function $\boldsymbol{\omega}$ (see (3)) is upper bounded by $\frac{\sqrt{2}}{2}\gamma$, i.e.,

$$\|\boldsymbol{\omega}(\mathbf{x}, t)\| \leq \frac{\sqrt{2}}{2}\gamma. \tag{13}$$

C3) the function $V(\mathbf{x}, t) = \mathbf{x}^\top \mathbf{P}_\varepsilon(t)\mathbf{x}$ decreases along the direction $\boldsymbol{\mu}$ in the sense that inequality

$$V(\mathbf{x}, t) \geq V(\boldsymbol{\mu}(\mathbf{x}, t), t), \tag{14}$$

holds in the domains of V.

Under these conditions, the following theorem is presented.

Theorem 2.1: [11, Theorem 3] Let conditions C1-C3 be satisfied with some $\gamma > 0$. Then the closed-loop system driven by the state feedback

$$\mathbf{u} = -\mathbf{g_2}(\mathbf{x}, t)^\top \mathbf{P}_\varepsilon(t)\mathbf{x} \tag{15}$$

locally possesses a $\mathcal{L}_2$-gain less than γ. Moreover, the disturbance-free closed-loop system (1)-(4), (15) is uniformly asymptotically stable.

For the periodic tracking of period T with periodic impact instants $t_{i+1} = t_i + T,\ i = 1, 2, \ldots$, Theorem 2.1 admits a time-periodic synthesis (15) which is based on an appropriate periodic solution $\mathbf{P}_\varepsilon(t)$ of the periodic differential Riccati equation (12). It should be noted that $P_\varepsilon(t_{i+1}^+) = P_\varepsilon(t_i^+)$, due to the periodicity, and inequality (14) of C3 is then specified to the boundary condition

$$\mathbf{x}^\top \mathbf{P}_\varepsilon(t_2^-)\mathbf{x} \geq \boldsymbol{\mu}^\top(\mathbf{x}, t_1^+))\mathbf{P}_\varepsilon(t_1^+)\boldsymbol{\mu}(\mathbf{x}, t_1^+)), \tag{16}$$

on the Riccati equation (12).

This result will be used in the following section to robustly track a reference trajectory for a fully actuated 3D biped robot.

III. Robust trajectory tracking of a 3D Biped Robot

In this sections, the results on $\mathcal{H}_\infty$ control of mechanical systems under unilateral constraints are implemented on the 32-DOF biped robot ROMEO, from Aldebaran Robotics. In order to comply with all the conditions for the existence of the controller, an online trajectory adaptation method is introduced so as to ensure asymptotic tracking of the biped dynamics to the desired walking gait.

A. Model of a biped with feet

The bipedal robot considered in this section is walking on a rigid and horizontal surface. It consists of the 32-DOF robot Romeo, of Aldebaran Robotics, depicted in Fig. 1. The walking gait takes place in the sagittal plane and is composed of single support phases and impacts. The complete model of the biped robot consists of two parts: the differential equations describing the dynamics of the robot during the swing phase, and an impulse model of the contact event.

Fig. 1: 32-DOF Robot Romeo, of Aldebaran Robotics

1) Dynamic model in a single support: In the single support phase, considering a flat foot contact of the stance foot with the ground (i.e. there is no take off, no rotation, and no sliding during this phase), the dynamic model of the biped can be written as follows:

$$\mathbf{D}(\mathbf{q})\ddot{\mathbf{q}} + \mathbf{H}(\mathbf{q}, \dot{\mathbf{q}}) = \mathbf{D}_{\mathbf{\Gamma}}\mathbf{\Gamma} + \mathbf{w} \tag{17}$$

with $\mathbf{q} = (q_1, q_2, \ldots, q_{32})^\top$ the 32×1 vector of generalized coordinates, $\mathbf{D}$ is the symmetric, positive definite 32×32 inertia matrix, $\mathbf{D}_{\mathbf{\Gamma}}$ is a 32×32 constant and nonsingular matrix; $\mathbf{\Gamma} = (\Gamma_1, \ldots, \Gamma_{32})^\top$ is the 32×1 vector of joint torques; the term $\mathbf{H}(\mathbf{q}, \dot{\mathbf{q}})$ is the 32×1 vector of the centrifugal, coriolis and gravity forces; and $\mathbf{w}$ is the 32×1 vector of external disturbances.

2) Impact model: Now, assuming a flat foot contact, the double support phase is instantaneous and it can be modeled through passive impact equations, $i.e.$ impulsive torques are applied in the interlink joints ([16]). An impact appears at a time $t = T_I$ when the swing leg touches the ground. We shall assume that the impact is passive, absolutely inelastic, and that the legs do not slip ([17]). Given these conditions, the ground reactions can be viewed as impulsive forces. The algebraic equations, allowing one to compute the jumps of the velocities, can be obtained through integration of the dynamic equations of the motion, taking into account the ground reactions during an infinitesimal time interval from T_I^- to T_I^+ around an instantaneous impact. The torques supplied by the actuators at the joints, the centrifugal, Coriolis and gravity forces have finite values, thus not influencing an impact.

The impact is assumed to be with complete surface of the foot sole touching the ground. This means that the velocity of the swing foot impacting the ground is zero after impact. After an impact, the right foot (previous stance foot) takes off the ground, so the vertical component of the velocity of the taking-off foot just after an impact must be directed upwards and the impulsive ground reaction in this foot equals zeros. Thus, the impact dynamic model can be represented in the form ([18]):

$$\dot{\mathbf{q}}^+ = \phi(\mathbf{q})\dot{\mathbf{q}}^- + \mathbf{w_d} \tag{18}$$

where $\dot{\mathbf{q}}^-$ is the velocity of the robot before the impact and $\dot{\mathbf{q}}^+$ is the velocity after the impact; $\phi(\mathbf{q})$ represents a restitution law that determines the relations between the velocities before and after the impacts; $\mathbf{q}$ is the position at the impact. The additive term $\mathbf{w_d}$ is introduced to account for inadequacies in this restitution law.

The unilateral constraint can be defined as $\mathbf{F}(\mathbf{q})$, which represents the height of swing foot, as a function of the generalized coordinates of the implicit-contact model (17). In the next section, a specific trajectory invoked to generate a cyclic motion of the undisturbed model (17)-(18), is designed so it can be used in our tracking problem as a reference trajectory.

B. Motion Planning

Since a walking biped gait is a periodical phenomenon, the objective is to design a cyclic biped gait. A complete walking cycle is composed of two phases: a single support phase, and an instantaneous support phase, which is modeled through passive impact equations. The single support phase has a duration of $0.31\ s$, and it begins with one foot which stays on the ground while the other foot swings from the rear to the front. The double support phase is assumed instantaneous. This means that when the swing leg touches the ground the stance leg takes off. The reference trajectories, allowing a symmetric step, are obtained by an off-line optimization, minimizing a Sthenic criteria, as presented in the work of [17]. The restitution law during the impact phase is given by:

$$\dot{\mathbf{q}}_\mathbf{d}(t_k^+) = \phi(\mathbf{q}_\mathbf{d}(t_k))\dot{\mathbf{q}}_\mathbf{d}(t_k^-), \quad k = 1, 2, \ldots. \tag{19}$$

C. Pre-feedback desing

Our objective is to design a pre-feedback controller of the form

$$\mathbf{\Gamma} = \mathbf{D_\Gamma}^{-1}[\mathbf{D}(\ddot{\mathbf{q}}_\mathbf{d} + \mathbf{u}) + \mathbf{H}] \tag{20}$$

that imposes on the undisturbed biped motion desired stability properties around $\mathbf{q_d}$ while also locally attenuating the effect of the disturbances. Thus, the controller to be constructed consists of the feedback linearizing terms of (20) subject to $\mathbf{u} = \mathbf{0}$, which are responsible for the trajectory compensation, and a disturbance attenuator $\mathbf{u}$, internally stabilizing the closed-loop system around the desired trajectory. In what follows, we confine our research to the trajectory tracking control problem where the output to be controlled is given by

$$\mathbf{z} = \begin{bmatrix} \mathbf{0} \\ \rho_p(\mathbf{q_d} - \mathbf{q}) \\ \rho_v(\dot{\mathbf{q}}_\mathbf{d} - \dot{\mathbf{q}}) \end{bmatrix} + \begin{bmatrix} \mathbf{1} \\ \mathbf{0} \\ \mathbf{0} \end{bmatrix} \mathbf{u} \tag{21}$$

$$\mathbf{z_d} = \mathbf{q_d}(t_k^+) - \mathbf{q}(t_k^+) \tag{22}$$

with positive weight coefficients ρ_p, ρ_v.

Now, let us introduce the state deviation vector $\mathbf{x} = (\mathbf{x}_1, \mathbf{x}_2)^\top$, where $\mathbf{x}_1(t) = \mathbf{q_d}(t) - \mathbf{q}(t)$ is the position deviation from the desired trajectory, and $\mathbf{x}_2(t) = \dot{\mathbf{q}}_d(t) - \dot{\mathbf{q}}(t)$ is the velocity deviation from the desired velocity.

Then, rewriting the state equations (17)-(22) in terms of the errors $\mathbf{x_1}$ and $\mathbf{x_2}$, we obtain an error system in the form (1)-(4), being specified with

$$\mathbf{f}(\mathbf{x}, t) = \begin{bmatrix} \mathbf{x}_2 \\ \mathbf{0} \end{bmatrix}, \mathbf{g_1}(\mathbf{x}, t) = \begin{bmatrix} \mathbf{0} \\ \mathbf{D^{-1}}(\mathbf{q_d} - \mathbf{x_1}) \end{bmatrix}, \tag{23}$$

$$\mathbf{g_2}(\mathbf{x}, t) = \begin{bmatrix} \mathbf{0} \\ \mathbf{I} \end{bmatrix}, \mathbf{h}(\mathbf{x}) = \begin{bmatrix} \mathbf{0} \\ \rho_p \mathbf{x}_1 \\ \rho_v \mathbf{x}_2 \end{bmatrix}, \mathbf{k_{12}}(\mathbf{x}) = \begin{bmatrix} \mathbf{I} \\ \mathbf{0} \\ \mathbf{0} \end{bmatrix}, \tag{24}$$

$$\mu(\mathbf{x}, t) = \begin{bmatrix} \mathbf{x_1} \\ \phi(\mathbf{q_d})\dot{\mathbf{q}}_\mathbf{d} - \phi(\mathbf{q_d} - \mathbf{x_1})(\dot{\mathbf{q}}_\mathbf{d} - \mathbf{x_2}) \end{bmatrix}, \tag{25}$$

$$\omega(\mathbf{x}, t) = -\mathbf{I} \tag{26}$$

where as a matter of fact, the zero symbols stand for zero matrices and $\mathbf{I}$ for identity matrices of appropriate dimensions.

D. State Feedback $\mathcal{H}_\infty$ Synthesis Using Trajectory Adaptation

To respect Condition C1 of Theorem 2.1 for the error system (1)-(4), the controlled output (21) is specified with $\rho_p = 3500$ and $\rho_v = 500$, and then, following the standard $\mathcal{H}_\infty$ design procedure (see, e.g., [15, Section 6.2.1]), the disturbance attenuation level and the perturbation parameter are set to $\gamma = 200$ and $\epsilon = 0.01$ to ensure an appropriate solvability of the perturbed differential Riccati equation (12), subject to the boundary condition (16). Next, condition C2 of Theorem 2.1 is then straightforwardly verified with γ, thus specified, and with $\boldsymbol{\omega}$, being an identity matrix. Finally, to comply with condition C3 of Theorem 2.1 to be verified at the impact time instants, the previously defined reference trajectory, is adapted on-line in such a manner that the state error dynamics possess no jumps. Thus, inequality (14) becomes redundant for the adapted trajectory because only trivial transitions with $\boldsymbol{\mu}(\mathbf{x},t) = 0$ are feasible.

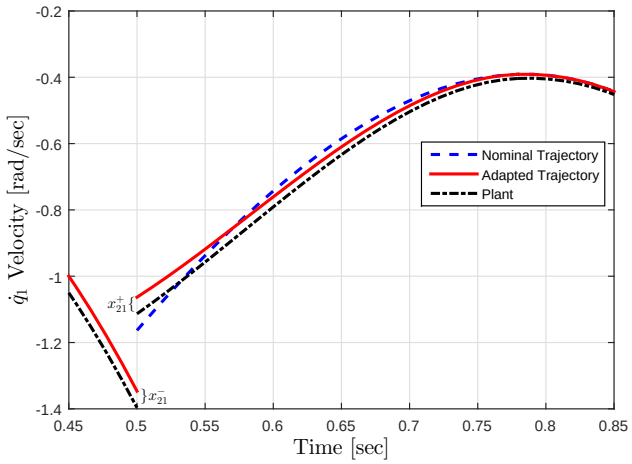

Fig. 2: Reference velocity adaptation for the first joint, with an impact at $t^l = 0.5$. After the impact, the initial value of the adapted velocity is such that the pre-impact ($x_{21}(t^l-) = \dot{q}_1(t^l-) - \dot{q}_1^r(t^l-)$) and post-impact ($x_{21}(t^l+) = \dot{q}_1(t^l+) - \dot{q}_1^r(t^l+)$) tracking errors are the same, and at the middle of the step, the adapted reference velocity reaches the nominal one.

For hybrid systems with state-triggered jumps, the jump times of the plant and the reference trajectory are in general not coinciding. During the time interval caused by this

jump-time mismatch, the tracking error is large, even in the undisturbed case. Since this behavior also occurs for arbitrarily small initial errors, the error dynamic displays unstable behavior in the sense of Lyapunov. This behavior is known in the literature as "peaking". It is expected to occur in all hybrid systems with state-triggered jumps when considering tracking or observer design problems [19], and imposes a difficulty in guaranteeing that the norm of the tracking error converges to zero. In order to achieve synchronization in our biped application, the reference trajectory is adapted, as illustrated in Fig.2 for the first joint q_1. Provided that the impact is detectable (e.g., by using a force or touch sensor) it happens that either the reference trajectory hits the constraint before the plant does, or the plant hits the constraint before the reference trajectory does. In the former scenario, the reference trajectory is continuously extrapolated until the plant collision occurs whereas in the latter scenario, the reference trajectory is restarted on-line once the plant collision is detected. Either way, both the plant trajectory and the adapted reference trajectory exhibit impacts at the same time instants. By adaptation, the nominal reference trajectory, and the adapted one, are equivalent before a collision. The position and velocity tracking errors are measured, and once the impact of the plant is detected, the adapted trajectory is updated on-line in such a manner that the new post-impact error, x_{21}^{+} in Fig.2, coincides with the error measured before the impact ($x_{21}(t^{l}-)$ in Fig.2), thereby rendering the evolution of the error to exhibit no jump, so as to ensure a smooth control action. Following the idea of [20], a new polynomial is defined for the adapted trajectory, that starts from this imposed condition, and will join the nominal reference trajectory at the middle of the step with the same velocity, and will continue to be the same until the end of the step. While the reference trajectory is recalculated after the impact, the perturbed differential Riccati equation (12) is also updated, and its corresponding solution is recomputed on-line.

E. Numerical study

To illustrate the performance issues of the developed stable bipedal gait synthesis numerical simulations were performed for a laboratory prototype whose parameters were drawn from the Aldebaran's ROMEO documentation. The contact constraints (no-take off, no rotation, and no sliding during the single support phase) are verified on-line to confirm the validity of (17), (18). The well-known constraint (complementarity)-based approach [21], [22], [23] is utilized to simulate the biped contact with the ground. The latter approach belongs to the family of time-stepping approaches and it is often invoked for biped dynamics simulations (see, e.g., the works by [24], [25], [26]).

It can be seen that these joints possess a periodic trajectory. Figure 3 depicts the resulting heights of the feet for the undisturbed case, when the plant initial conditions are deviated a 5% from the reference gait's initial conditions. As presented for the planar biped, the periodicity of these heights is a good indicator of a stable motion for the walking gait. In Fig.3, legends "P1" and "P4" represent the corners corresponding to the "toe" of the foot, whereas "P2" and "P3" represent the corners of the "heel" of the foot. As predicted by the theory, Figure 4 depicts the Lyapunov function $V(\mathbf{x}, t)$, decreasing smoothly and asymptotically towards zero, so the robot gait converges asymptotically to the desired gait. Furthermore, Figs. 5-6 depict the zero moment point (ZMP) locations and ground reactions for both feet, which are verified to comply with the contact constraints.

As a next step, a persistent disturbance of $F_w = 10\sin(t)\ Nm$ was applied to the hip (therefore vector $\mathbf{w}$ is given by the joint torques generated by this external force), while the velocities after the impact are deviated $5\ \%$ from their nominal values (given by (19), so $\mathbf{w_d} = 0.05\phi(\mathbf{q})\dot{\mathbf{q}}^{-}$), thus considering disturbances on both the single support and impact phases. Six joints among the 32 were selected to clearly illustrate the effect of this disturbance (both ankles, knees, and hip joints). This is depicted in Fig. 7, where the error is small and bounded, and the robot maintains a stable walking gait. The torques for these joints are shown in Fig. 8, where they stay between the buondaries of $\pm 150\ Nm$. Despite the disturbances, good performance of the closed-loop error dynamics, driven by the proposed nonlinear $\mathcal{H}_\infty$ state feedback, is still achieved.

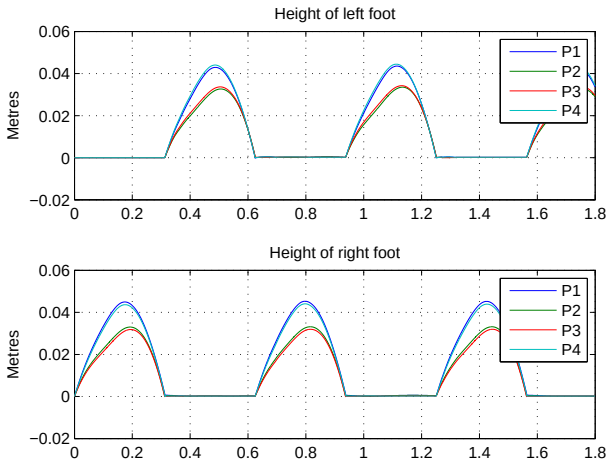

Fig. 3: Feet heights for 6 steps for Romeo, representing a stable motion

Finally, the performance of the $\mathcal{H}_\infty$ controller was compared against the performance of a PD controller. In order to do a fair comparison, the same pre-feedback (20) was used, and just the disturbance attenuator (15) was replaced by the PD controller $\mathbf{u} = -\mathbf{K_p x_1} - \mathbf{K_v x_2}$, with the constant matrices $[\mathbf{K_p}, \mathbf{K_v}] = \mathbf{B_2^\top P}_\varepsilon$ where $\mathbf{P}_\varepsilon$ is the solution of the algebraic version of the Riccati equation (12) with $\dot{\mathbf{P}}_\varepsilon = \mathbf{0}$.

The comparison results with the time-varying disturbance force $10\sin(t)+10\ N$, applied to the hip are shown in Fig.9, where it can be seen that after $6.13\ s$, the cumulative position tracking error, generated by the developed nonlinear periodic $\mathcal{H}_\infty$ tracking controller, is approximately 26% less than that generated by the PD controller. Thus, a better performance

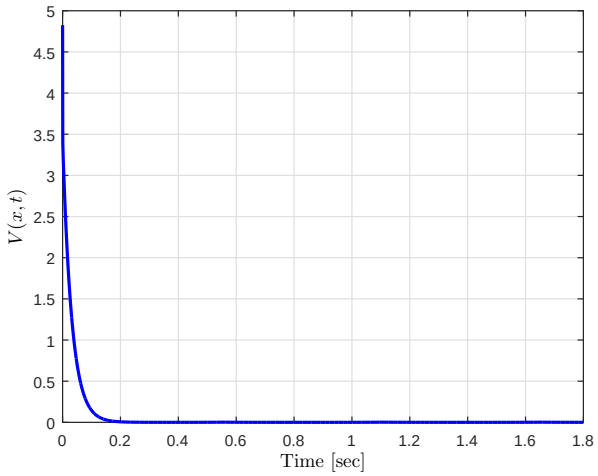

Fig. 4: Lyapunov function for the undisturbed system, with nonzero initial conditions.

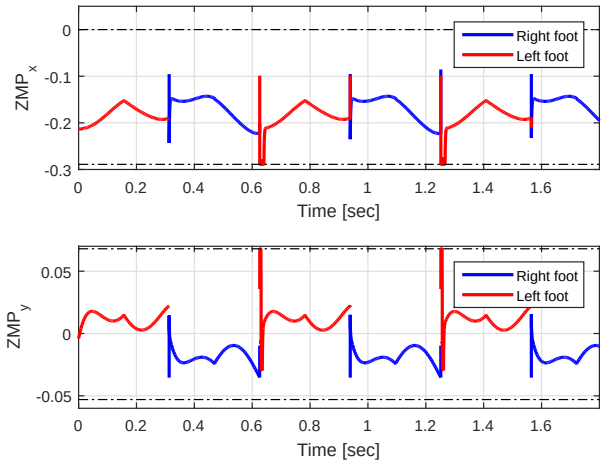

Fig. 5: Zero moment point locations for both feet during the disturbance free walking gait. The dashed lines represent the feet geometrical limits and the ZMP always rests inside of them, thus illustrating no rotation of the support foot at each step.

of the proposed synthesis is concluded in comparison to the standard linear $\mathcal{H}_\infty$ PD design coupled to the pre-feedback linearization.

IV. Conclusion

In this paper, the state feedback $\mathcal{H}_\infty$-control synthesis under unilateral constraints was implemented on a 3D fully actuated biped robot. In order to guarantee asymptotic stability of the hybrid error dynamics, an online trajectory adaptation scheme was utilized, so as to prevent the peaking phenomena that appears in the tracking of hybrid systems with state-triggered jumps. The combination of the robust synthesis with the trajectory adaptation constitutes the contribution of the paper. Effectiveness of the resulting design procedure is supported by numerical tests on the 32-DOF biped robot

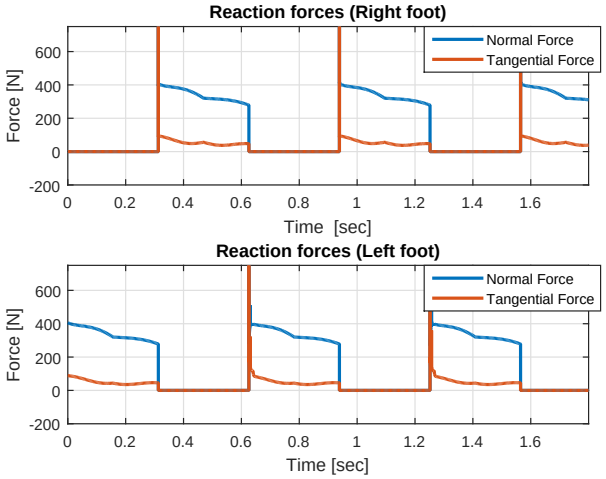

Fig. 6: Ground reactions during the disturbance free walking gait.

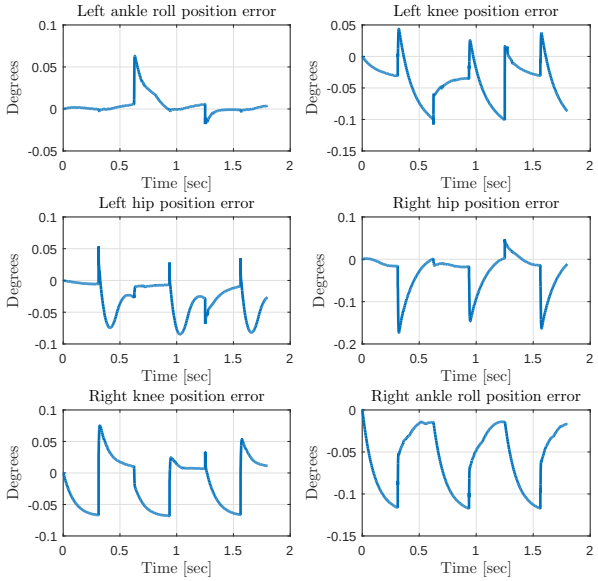

Fig. 7: Joints errors for left and right hips, knees, and ankles, under a persistent continuous disturbance $(10\sin(t)\ Nm)$ applied on the hip.

ROMEO, exhibiting the desired disturbance attenuation in the presence of disturbances in the single support phase and uncertainty in the impact phase.

References

[1] E. Westervelt, J. Grizzle, C. Chevallereau, J. Choi, and B. Morris, *Feedback control of dynamic bipedal robot locomotion*. CRC press Boca Raton, 2007.

[2] H. Dai and R. Tedrake, "$\mathcal{L}_2$-gain optimization for robust bipedal walking on unknown terrain," in *Robotics and Automation (ICRA), 2013 IEEE International Conference on*. IEEE, 2013, pp. 3116–3123.

[3] K. Hamed and J. Grizzle, "Robust event-based stabilization of periodic orbits for hybrid systems: Application to an underactuated 3d bipedal

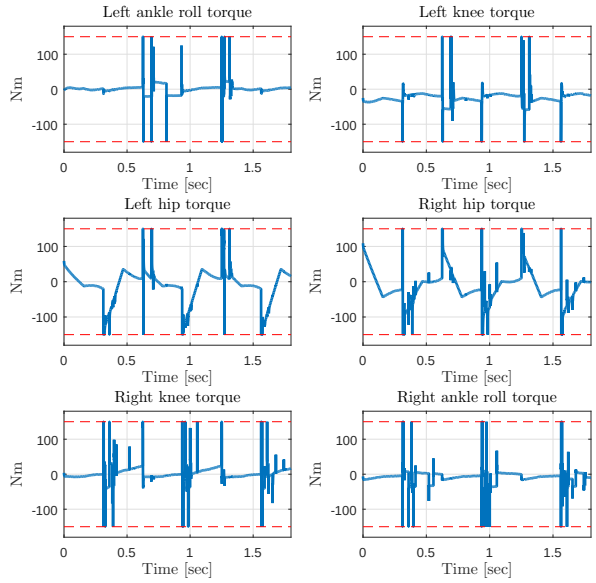

Fig. 8: Torques for left and right hips, knees, and ankles, under a persistent continuous disturbance $(10\sin(t)\ Nm)$ applied on the hip.

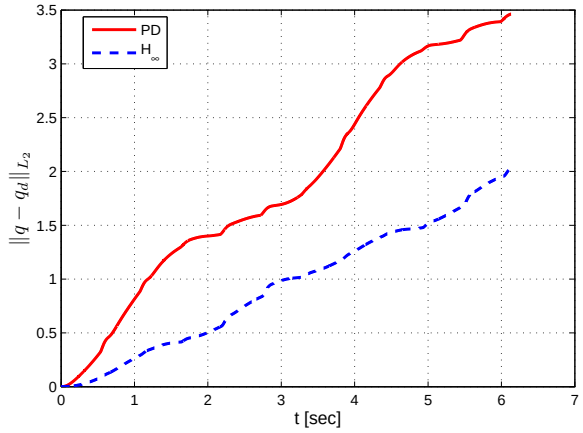

Fig. 9: Cumulative error comparison of the nonlinear $\mathcal{H}_\infty$ controller (solid lines) vs. the linear $\mathcal{H}_\infty$ PD controller (dashed lines).

robot," in *Proceedings of the 2013 American Control Conference*, 2013.

[4] R. Goebel, R. Sanfelice, and A. Teel, "Hybrid dynamical systems," *Control Systems, IEEE*, vol. 29, no. 2, pp. 28–93, 2009.

[5] W. Haddad, N. Kablar, V. Chellaboina, and S. Nersesov, "Optimal disturbance rejection control for nonlinear impulsive dynamical systems," *Nonlinear Analysis: Theory, Methods & Applications*, vol. 62, no. 8, pp. 1466–1489, 2005.

[6] D. Nesic, L. Zaccarian, and A. Teel, "Stability properties of reset systems," *Automatica*, vol. 44, no. 8, pp. 2019–2026, 2008.

[7] N. Manamani, N. Gauthier, and N. MSirdi, "Sliding mode control for pneumatic robot leg," in *Proceedings European Control Conference*, 1997.

[8] M. Nikkhah, H. Ashrafiuon, and F. Fahimi, "Robust control of underactuated bipeds using sliding modes," *Robotica*, vol. 25, no. 03, pp. 367–374, 2007.

[9] Y. Aoustin, C. Chevallereau, and Y. Orlov, "Finite time stabilization of a perturbed double integrator-part ii: applications to bipedal locomotion," in *Decision and Control (CDC), 2010 49th IEEE Conference on*. IEEE, 2010, pp. 3554–3559.

[10] H. Oza, Y. Orlov, S. Spurgeon, Y. Aoustin, and C. Chevallereau, "Finite time tracking of a fully actuated biped robot with pre-specified settling time: a second order sliding mode synthesis," in *Robotics and Automation (ICRA), 2014 IEEE International Conference on*. IEEE, 2014, pp. 2570–2575.

[11] O. Montano, Y. Orlov, and Y. Aoustin, "Nonlinear $h\infty$-control under unilateral constraints," *International Journal of Control*, pp. 1–23, 2016.

[12] A. Robotics, "Project romeo," www.ald.softbankrobotics.com/fr/cool-robots/romeo, 2016, accessed: 2016-07-01.

[13] B. Brogliato, S. Niculescu, and P. Orhant, "On the control of finite-dimensional mechanical systems with unilateral constraints," *Automatic Control, IEEE Transactions on*, vol. 42, no. 2, pp. 200–215, 1997.

[14] Y. Orlov, *Discontinuous systems–Lyapunov analysis and robust synthesis under uncertainty conditions*. Springer, 2009.

[15] Y. Orlov and L. Aguilar, *Advanced $\mathcal{H}_\infty$ Control–Towards Nonsmooth Theory and Applications*. Birkhauser:Boston, 2014.

[16] A. M. Formalskii, "Ballistic walking design via impulsive control," *Journal of Aerospace Engineering*, vol. 23, no. 2, pp. 129–138, 2009.

[17] D. Tlalolini, Y. Aoustin, and C. Chevallereau, "Design of a walking cyclic gait with single support phases and impacts for the locomotor system of a thirteen-link 3d biped using the parametric optimization," *Multibody System Dynamics*, vol. 23, no. 1, pp. 33–56, 2010.

[18] A. Haq, Y. Aoustin, and C. Chevallereau, "Effects of knee locking and passive joint stiffness on energy consumption of a seven-link planar biped," in *Robotics and Automation (ICRA), 2012 IEEE International Conference on*. IEEE, 2012, pp. 870–876.

[19] J. Biemond, N. van de Wouw, W. Heemels, and H. Nijmeijer, "Tracking control for hybrid systems with state-triggered jumps," *Automatic Control, IEEE Transactions on*, vol. 58, no. 4, pp. 876–890, 2013.

[20] A. Grishin, A. Formalsky, A. Lensky, and S. Zhitomirsky, "Dynamic walking of a vehicle with two telescopic legs controlled by two drives," *The International Journal of Robotics Research*, vol. 13, no. 2, pp. 137–147, 1994.

[21] C. Rengifo, Y. Aoustin, F. Plestan, C. Chevallereau, *et al.*, "Contact forces computation in a 3d bipedal robot using constrained-based and penalty-based approaches," *Proceedings of Multibody Dynamics*, 2011.

[22] V. Acary and B. Brogliato, *Numerical methods for nonsmooth dynamical systems: applications in mechanics and electronics*. Springer, 2008, vol. 35.

[23] B. Brogliato, *Impacts in mechanical systems: analysis and modelling*. Springer Verlag, 2000, vol. 551.

[24] P. Van Zutven, D. Kostic, and H. Nijmeijer, "On the stability of bipedal walking," *Simulation, Modeling, and Programming for Autonomous Robots*, p. 521, 2010.

[25] Y. Hurmuzlu, F. Génot, and B. Brogliato, "Modeling, stability and control of biped robotsa general framework," *Automatica*, vol. 40, no. 10, pp. 1647–1664, 2004.

[26] K. Yunt and C. Glocker, "Trajectory optimization of mechanical hybrid systems using sumt," in *9th IEEE International Workshop on Advanced Motion Control*. IEEE, 2005, pp. 665–671.